Charge form factor of ^{7}Li with resonating-group wave function

H. Kanada
School of Physics, University of Minnesota, Minneapolis, Minnesota 55455
and Department of Physics, Niigata University, Niigata, Japan † †

Q. K. K. Liu
School of Physics, University of Minnesota, Minneapolis, Minnesota 55455 †
and Hahn-Meitner-Institut für Kernforschung, Berlin, Germany †

Y. C. Tang
School of Physics, University of Minnesota, Minneapolis, Minnesota 55455

(Received 28 February 1980)

The charge form factor of ^{7}Li in the q^2 range of 0 to 7 fm^{-2} is calculated with a single-channel $t+\alpha$ resonating-group wave function which is fully antisymmetric and treats correctly the motion of the total center of mass. Both $C0$ and $C2$ contributions are taken into account, and proton and neutron distributions are separately considered. With no adjustable parameters in the calculation, the result obtained shows that a good agreement between theory and experiment can be achieved. The calculated rms charge radius and spectroscopic quadrupole moment are equal to 2.44 fm and -3.70 fm^2, respectively, which agree very well with empirically determined values.

[NUCLEAR STRUCTURE ^{7}Li; charge form factor with resonating-group wave function.]

I. INTRODUCTION

The resonating-group method, described thoroughly in various reviews[1-4] and representative articles,[5-8] has been extensively used to study bound-state, scattering, and reaction problems in light and medium nuclear systems. With the adoption of rather realistic nucleon-nucleon potentials, it was found that satisfactory agreement with experiment for bound-state energies and scattering and reaction cross sections can generally be obtained. As has been emphasized previously,[1,2] this is a method based on the cluster representation of the nucleus and distinguished by the important facts that in its formulation totally antisymmetric many-nucleon wave functions are used and the center-of-mass motion is correctly taken into consideration. Consequently, nucleon-exchange effects, which are especially significant when the interacting clusters have similar mass, are fully accounted for and, unlike some other types of existing calculations, undesirable features associated with improper treatment of the c.m. degree of freedom are not present in resonating-group investigations.

Because of the requirements of total antisymmetrization and translational invariance of the wave function, resonating-group calculations are frequently rather tedious to perform. As a consequence, many studies employing this method have been carried out by including only a small number of cluster configurations in the formulation. For example, for the description of the ground and low excited states in the nucleus ^{20}Ne,[9-12] most existing calculations have only taken a single cluster configuration, namely, the $\alpha+^{16}$O cluster configuration, into consideration. The results obtained were, however, still quite satisfactory, which is connected with the fact[1] that, especially in light systems, clustering effects are prominent and, thus, even such simplified single-channel calculations can be expected to yield reliable information.

To study the general utility of the resonating-group wave function, we calculate in this investigation the charge form factor of ^{7}Li by using the ground-state wave function obtained by Furber[13] in a single-channel $t+\alpha$ resonating-group calculation. We choose this particular system for a detailed examination, not only because ^{7}Li is an interesting nucleus possessing a large quadrupole moment, but also because there is ample evidence for strong clustering in the ground state and, hence, a single-channel $t+\alpha$ calculation should be sufficient to explain the essential behavior of this nucleus. Indeed, with a nucleon-nucleon potential containing both central and spin-orbit components, it was found by Furber that it is possible to obtain a good agreement not only with the bound-state data but also with empirical phase-shift results in the low-energy region.[14] Therefore, one anticipates that the many-nucleon wave function resulting from this single-channel calculation is adequate and one will be able to learn from the form-factor

calculation some important features associated with the structure of the ^{7}Li nucleus.

A previous analysis of the ^{7}Li charge form-factor data was undertaken by Suelzle *et al.*[15] using a $(1s)^4(1p)^3$ oscillator model. By adjusting the oscillator width parameter and the magnitude of the electric quadrupole moment, a good agreement with experiment has been obtained. We should point out, however, that the ^{7}Li wave function used by these authors does not follow in any clear manner from basic nucleon-nucleon interactions and the adjustment of the quadrupole moment is an internally inconsistent procedure. In contrast, the wave function we adopt here is the direct result of a strong-interaction study and there are *no* adjustable parameters in our form-factor calculation.

In Sec. II, we give a brief description of the ^{7}Li resonating-group wave function and discuss the formulation of the form-factor problem. Both $C0$ and $C2$ contributions from proton and neutron distributions will be taken into consideration. The results are presented in Sec. III. Here we shall see that the proton and neutron distributions have rather different characteristics and, hence, the charge form factor of ^{7}Be, if measurable, would turn out to be appreciably different from that of ^{7}Li. Finally, in Sec. IV, we summarize the findings of this investigation and mention other interesting calculations which are worth performing if one wishes to understand better the properties of the seven-nucleon system.

II. FORMULATION

A. Brief description of the resonating-group wave function

The formulation of a $t+\alpha$ resonating-group calculation is described in Ref. 13 and Sec. 5.5 of Ref. 1; hence, only a very brief discussion will be given here. In the single-channel approximation, the wave function is written as

$$\psi_M = \mathcal{A}\bar{\psi}_M, \tag{1}$$

where $\mathcal{A}$ is an antisymmetrization operator and

$$\bar{\psi}_M = \phi_\alpha \phi_t \left[\frac{1}{R} f_{Jl}(R) \mathcal{Y}^M_{Jls}\right] Z(\vec{R}_{\text{c.m.}}). \tag{2}$$

The function $\mathcal{Y}^M_{Jls}$ is a spin-isospin-angle function, appropriate for $T=\frac{1}{2}$, $S=\frac{1}{2}$, and required values of orbital angular momentum l and total angular momentum J with z component M; its explicit form is

$$\mathcal{Y}^M_{Jls} = \sum_\mu C(lSJ;\, \mu, M-\mu, M) Y^\mu_l(\hat{R}) \xi^{M-\mu}_s, \tag{3}$$

with $C(lSJ;\, \mu, M-\mu, M)$ being a Clebsch-Gordan coefficient in the notation of Rose,[16] and $\xi^{M-\mu}_s$ being a spin-isospin function having $(M-\mu)$ for the z component of the spin angular momentum. Also, the functions ϕ_α and ϕ_t represent the internal spatial structures of the α and t clusters, respectively; they are assumed to have the normalized forms

$$\phi_\alpha = \left(\frac{\alpha_A^3}{4\pi^3}\right)^{3/4} \exp\left[-\tfrac{1}{2}\alpha_A \sum_{i=1}^{4} (\vec{r}_i - \vec{R}_\alpha)^2\right], \tag{4}$$

$$\phi_t = \left(\frac{\alpha_B^2}{3\pi^2}\right)^{3/4} \exp\left[-\tfrac{1}{2}\alpha_B \sum_{i=5}^{7} (\vec{r}_i - \vec{R}_t)^2\right], \tag{5}$$

where $\vec{R}_\alpha$ and $\vec{R}_t$ denote, respectively, the c.m. coordinates of the two clusters. The values of the width parameters α_A and α_B used are[17]

$$\alpha_A = 0.514 \text{ fm}^{-2}, \tag{6}$$

$$\alpha_B = 0.378 \text{ fm}^{-2}. \tag{7}$$

These particular values are chosen in order to yield correct α-particle and triton rms matter radii in accordance with data from electron-scattering experiments. Finally, in Eq. (2), the function $Z(\vec{R}_{\text{c.m.}})$ describes the c.m. motion of the entire system. It can be chosen as any normalizable function; however, in the present calculation where the complex-generator-coordinate technique (CGCT)[2,18] is used, we shall, for ease in analytical computation, choose it as

$$Z(\vec{R}_{\text{c.m.}}) = \left(\frac{N_A\alpha_A + N_B\alpha_B}{\pi}\right)^{3/4} \times \exp\left[-\tfrac{1}{2}(N_A\alpha_A + N_B\alpha_B)\vec{R}^2_{\text{c.m.}}\right], \tag{8}$$

with $N_A=4$ and $N_B=3$ being the nucleon numbers of the α and t clusters, respectively.

The relative-motion function $f_{Jl}(R)$ is obtained by solving the projection equation

$$\langle \delta\psi_M | H - E_T | \psi_m \rangle = 0. \tag{9}$$

In the above equation, E_T is the total energy of the system and H is the Hamiltonian operator given by

$$H = \sum_{i=1}^{N} T_i + \sum_{i<j=1}^{N} V_{ij} - T_{\text{c.m.}}, \tag{10}$$

where $N = N_A + N_B$ and $T_{\text{c.m.}}$ is the kinetic-energy operator of the total center of mass. For the nucleon-nucleon potential V_{ij}, we utilize the one represented by Eq. (5.98) of Ref. 1 with $\lambda = 2.0$ fm^{-2}. In this potential, there exist an exchange-mixture parameter u in the central part and depth parameters V_λ and $V_{\lambda T}$ in the spin-orbit part. In the calculation of Furber,[13] the parameter u is fixed by considering the bound-state data of both ^{7}Li and ^{7}Be, while the parameters V_λ and $V_{\lambda T}$ are deter-

mined by adopting a best-fit procedure involving experimental data[19] for the energy splittings of the bound levels in ^{7}Li and ^{7}Be, and $p+\alpha$ and ^{3}He$+\alpha$ scattering in the low-energy region. For our present calculation, where our emphasis is to study the properties of ^{7}Li, we shall slightly modify Furber's results in order to reproduce precisely the experimental triton separation energies in the ground and first excited states of this nucleus. Thus, we use

$$u=0.983,$$
$$V_\lambda=-40 \text{ MeV}, \tag{11}$$
$$V_{\lambda\tau}=216 \text{ MeV}$$

in our present calculation. It should be mentioned that, with these values, even though the quality of fit to the $p+\alpha$ empirical phase-shift values is somewhat reduced, there is still a good agreement between calculated and experimental ^{3}He$+\alpha$ scattering results in the low-energy region.

The relative-motion function $f_{3/2,1}(R)$, or simply $f_G(R)$, for the ground state of ^{7}Li is depicted in Fig. 1. As has been emphasized previously,[1] one must be very careful in explaining the meaning of this function. Since it appears after the antisymmetrization operator in Eq. (1), it *cannot* be interpreted as proportional to the probability amplitude of finding the two clusters at a relative distance R with respect to each other. Because of this, it has been suggested by many authors[20-23] that, even for the modest purpose of constructing approximately an effective intercluster potential, one must not directly utilize the relative-motion

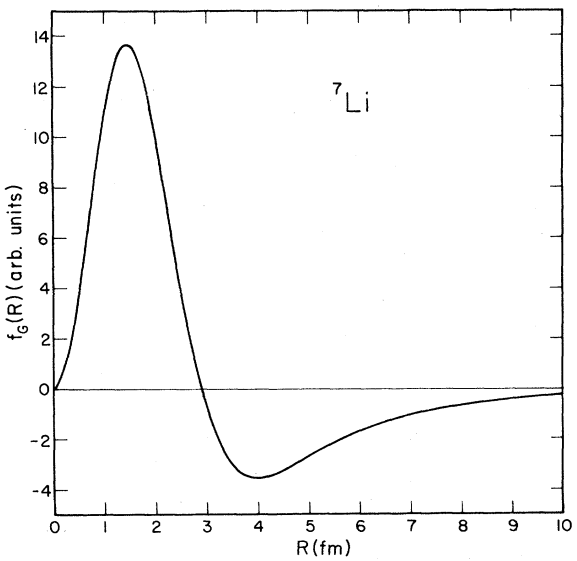

FIG. 1. Radial function $f_G(R)$ for the ground state of ^{7}Li with $l=1$ and $J=3/2$.

functions occurring in the resonating-group formulation, but should first perform a projection procedure by using the operator $\mathfrak{N}^{1/2}$, where $\mathfrak{N}$ represents the norm operator.[2]

B. Charge form factor of ^{7}Li

To calculate the charge form factor of ^{7}Li, we shall take both proton and neutron distributions into consideration. For this we first compute, in a definite magnetic substate, the bare form factors for proton and neutron distributions in the Born approximation given by

$$F_M^p=\frac{1}{N_p}\frac{\langle\bar{\psi}_M^G|\sum_{i=1}^{N}\exp[i\vec{q}\cdot(\vec{r}_i-\vec{R}_{c.m.})]\frac{1}{2}(1+\tau_{iz})|\psi_M^G\rangle}{\langle\bar{\psi}_M^G|\psi_M^G\rangle} \tag{12}$$

and

$$F_M^n=\frac{1}{N_n}\frac{\langle\bar{\psi}_M^G|\sum_{i=1}^{N}\exp[i\vec{q}\cdot(\vec{r}_i-\vec{R}_{c.m.})]\frac{1}{2}(1-\tau_{iz})|\psi_M^G\rangle}{\langle\bar{\psi}_M^G|\psi_M^G\rangle}. \tag{13}$$

In the above equations, $\vec{q}$ is the momentum transfer divided by $\hbar$, and N_p and N_n denote the proton and neutron numbers in ^{7}Li, respectively. The function ψ_M^G, with $\bar{\psi}_M^G$ being its unantisymmetrized part [see Eq. (1)], represents the ^{7}Li ground-state wave function, characterized by $l=1$ and $J=\frac{3}{2}$ with magnetic quantum number M. In defining the magnetic substates, we have chosen the quantization or z axis to be in the direction of the momentum transfer $\vec{q}$.

Upon averaging over initial magnetic substates and summing over final magnetic substates,[24] one obtains for the square of the charge form factor the expression

$$F_{ch}^2=\tfrac{1}{2}(F_{3/2}^2+F_{1/2}^2), \tag{14}$$

where[25]

$$F_{3/2}=F_{3/2}^p F_p+\frac{N_n}{N_p}F_{3/2}^n F_n, \tag{15}$$

$$F_{1/2}=F_{1/2}^p F_p+\frac{N_n}{N_p}F_{1/2}^n F_n, \tag{16}$$

with F_p and F_n being the charge form factors of the proton and the neutron, respectively. For these latter form factors, we use the values of Janssens *et al.*[26] given by

$$F_p=G_{ES}+G_{EV}, \tag{17}$$
$$F_n=G_{ES}-G_{EV}, \tag{18}$$

with

$$G_{ES}=0.5\left(\frac{2.50}{1+q^2/15.7}-\frac{1.60}{1+q^2/26.7}+0.10\right), \tag{19}$$

$$G_{EV}=0.5\left(\frac{1.16}{1+q^2/8.19}-0.16\right). \tag{20}$$

From $F_{3/2}$ and $F_{1/2}$, one obtains[24] the $C0$ charge form factor F_{C0} defined as

$$F_{C0}=\tfrac{1}{2}(F_{3/2}+F_{1/2}), \tag{21}$$

and the $C2$ charge form factor F_{C2} defined as

$$F_{C2}=\tfrac{1}{2}(F_{3/2}-F_{1/2}). \tag{22}$$

In terms of these form factors, one can further write $F_{\rm ch}^2$ as

$$F_{\rm ch}^2=F_{C0}^2+F_{C2}^2. \tag{23}$$

The mean-square charge radius $R_{\rm ch}^2$ and the spectroscopic quadrupole moment Q can then be determined by examining the low-q^2 behavior of F_{C0} and F_{C2}; these are given by[15]

$$R_{\rm ch}^2=-6\left(\frac{dF_{C0}}{dq^2}\right)_{q^2=0} \tag{24}$$

and

$$Q=-18\left(\frac{dF_{C2}}{dq^2}\right)_{q^2=0}. \tag{25}$$

From the above discussion, it is clear that the quantities we need to compute are the bare form factors F_M^p and F_M^n, with $M=\frac{3}{2}$ and $\frac{1}{2}$. To compute these quantities, we make use of the CGCT, which was especially developed for resonating-group studies involving clusters specified by *different* oscillator width parameters. This technique is well discussed in recent literatures[2,18,27,28] and, hence, will not be further described here.

Because of the fact that, in a resonating-group wave function, the c.m. function appears as a multiplicative factor, the expressions for F_M^p and F_M^n of Eqs. (12) and (13) may be readily simplified and become

$$F_M^p=\frac{1}{N_p}\frac{\langle\bar{\psi}_M^G|\sum_{i=1}^{N}\exp(i\vec{q}\cdot\vec{r}_i)\frac{1}{2}(1+\tau_{iz})|\psi_M^G\rangle}{\langle\bar{\psi}_M^G|\psi_M^G\rangle}\frac{1}{F_{\rm c.m.}} \tag{26}$$

and

$$F_M^n=\frac{1}{N_n}\frac{\langle\bar{\psi}_M^G|\sum_{i=1}^{N}\exp(i\vec{q}\cdot\vec{r}_i)\frac{1}{2}(1-\tau_{iz})|\psi_M^G\rangle}{\langle\bar{\psi}_M^G|\psi_M^G\rangle}\frac{1}{F_{\rm c.m.}}, \tag{27}$$

where

$$F_{\rm c.m.}=\langle Z|\exp(i\vec{q}\cdot\vec{R}_{\rm c.m.})|Z\rangle/\langle Z|Z\rangle. \tag{28}$$

With the c.m. function $Z(\vec{R}_{\rm c.m.})$ of Eq. (8), it can be easily shown that

$$F_{\rm c.m.}=\exp\left[-\frac{1}{4(N_A\alpha_A+N_B\alpha_B)}q^2\right]. \tag{29}$$

It should be emphasized that the appearance of the factor $F_{\rm c.m.}$ is a particular feature of the CGCT. As is seen from Eqs. (12) and (13), the c.m. degree of freedom is certainly taken into account in a correct manner in our present form-factor calculation.

With the use of the CGCT, the denominator $\langle\bar{\psi}_M^G|\psi_M^G\rangle$ in Eqs. (26) and (27) may be straightforwardly evaluated. The result is

$$\langle\bar{\psi}_M^G|\psi_M^G\rangle=\sum_{\mu}[C(lSJ;\mu,M-\mu,M)]^2\times\int G_\mu^*(\vec{R}')\mathcal{N}(\vec{R}',\vec{R}'')G_\mu(\vec{R}'')d\vec{R}'d\vec{R}'', \tag{30}$$

where

$$G_\mu(\vec{R}')=\frac{f_G(R')}{R'}Y_l^\mu(\hat{R}') \tag{31}$$

and $\mathcal{N}(\vec{R}',\vec{R}'')$ is the norm kernel[2] given by

$$\mathcal{N}(\vec{R}',\vec{R}'')=\mathcal{N}_0(\vec{R}',\vec{R}'')+\sum_{x=1}^{N_B}\mathcal{N}_x(\vec{R}',\vec{R}''), \tag{32}$$

with x ($1\leq x\leq N_B$, with $N_B<N_A$) being the number of nucleons interchanged between the α and t clusters. In Eq. (32), the functions $\mathcal{N}_0$ and $\mathcal{N}_x$ represent the direct and exchange parts of the norm kernel and have the forms

$$\mathcal{N}_0(\vec{R}',\vec{R}'')=\delta(\vec{R}'-\vec{R}''), \tag{33}$$

$$\mathcal{N}_x(\vec{R}',\vec{R}'')=(-1)^x\binom{N_B}{x}\frac{D_x}{D_0}\left(\frac{\pi^2}{a_xc_x}\right)^{3/2}\times\exp[-A_x(\vec{R}'^2+\vec{R}''^2)-C_x\vec{R}'\cdot\vec{R}''], \tag{34}$$

where

$$D_0=\left[\frac{16\pi^3N\alpha_A\alpha_B}{\mu_0^3(N_A\alpha_A+N_B\alpha_B)}\right]^{3/2}, \tag{35}$$

$$D_x=\left[\frac{4\alpha_A\alpha_B}{(\alpha_A+\alpha_B)^2}\right]^{3x/2}, \tag{36}$$

$$a_x=\frac{x}{4(\alpha_A+\alpha_B)}, \tag{37}$$

$$c_x=\frac{\Gamma_x}{N^2}\frac{N_A\alpha_A+N_B\alpha_B}{\alpha_A\alpha_B(\alpha_A+\alpha_B)}, \tag{38}$$

$$A_x=\frac{\mu_0^2}{4x\Gamma_x}\left\{x^2\left[(\alpha_A-\alpha_B)^2+\frac{2N}{\mu_0}\alpha_A\alpha_B\right]+N_AN_B\left(1-\frac{x}{\mu_0}\right)(\alpha_A+\alpha_B)^2\right\}, \tag{39}$$

$$C_x=-\frac{\mu_0^2}{2x\Gamma_x}\left[x^2(\alpha_A-\alpha_B)^2+N_AN_B\left(1-\frac{x}{\mu_0}\right)(\alpha_A+\alpha_B)^2\right], \tag{40}$$

with

$$\Gamma_x = N_A N_B(\alpha_A + \alpha_B) - x(N_A\alpha_A + N_B\alpha_B), \tag{41}$$

$$\mu_0 = N_A N_B/N. \tag{42}$$

It is worth mentioning that most of the formulas given in this article are quite general and can be applied to other two-cluster $A+B$ systems, with A and B being s-shell clusters.

The numerators of F_M^p and F_M^n can be similarly evaluated. They have the forms

$$\langle\bar{\psi}_M^G|\sum_{i=1}^{N}\exp(i\vec{q}\cdot\vec{r}_i)\tfrac{1}{2}(1+\tau_{iz})|\psi_M^G\rangle = \sum_{\mu}[C(lSJ;\mu,M-\mu,M)]^2 \times\int G_\mu^*(\vec{R}')I_p(\vec{R}',\vec{R}'')G_\mu(\vec{R}'')d\vec{R}'d\vec{R}'' \tag{43}$$

and

$$\langle\bar{\psi}_M^G|\sum_{i=1}^{N}\exp(i\vec{q}\cdot\vec{r}_i)\tfrac{1}{2}(1-\tau_{iz})|\psi_M^G\rangle = \sum_{\mu}[C(lSJ;\mu,M-\mu,M)]^2 \times\int G_\mu^*(\vec{R}')I_n(\vec{R}',\vec{R}'')G_\mu(\vec{R}'')d\vec{R}'d\vec{R}''. \tag{44}$$

In these equations, the interaction kernels I_p and I_n can again be separated into direct and exchange parts; in other words, one can write

$$\begin{aligned} I_p(\vec{R}',\vec{R}'') = {} & [2I_0^b + I_0^c] \\ & + [(I_1^{a1} + I_1^{a2}) + 5I_1^b + 2I_1^c] \\ & + [2(I_2^{a1} + I_2^{a2}) + 4I_2^b + I_2^c] \\ & + [(I_3^{a1} + I_3^{a2}) + I_3^b] \end{aligned} \tag{45}$$

and

$$\begin{aligned} I_n(\vec{R}',\vec{R}'') = {} & [2I_0^b + 2I_0^c] \\ & + [2(I_1^{a1} + I_1^{a2}) + 4I_1^b + 4I_1^c] \\ & + [4(I_2^{a1} + I_2^{a2}) + 2I_2^b + 2I_2^c] \\ & + [2(I_3^{a1} + I_3^{a2})]. \end{aligned} \tag{46}$$

On the right sides of the above equations, the subscript for I denotes the number of nucleons interchanged between the clusters, and the superscript represents the manner in which the longitudinal photon interacts with a particular nucleon in the clusters. As is seen, there are four interaction types, namely, types $a1$, $a2$, b, and c; these will be separately considered and discussed below.

To explain the origin of the four interaction types, we utilize the diagrammatical representation introduced by LeMere *et al.*[29] This is shown in Fig. 2, where each dot on the upper or lower line represents a particular spin and isospin state in the α or t cluster, and the solid-line exchange loop is used to indicate the nucleons which are interchanged between the clusters. By examining in detail the resonating-group formulation, one then finds that these interaction types arise in the following manner:

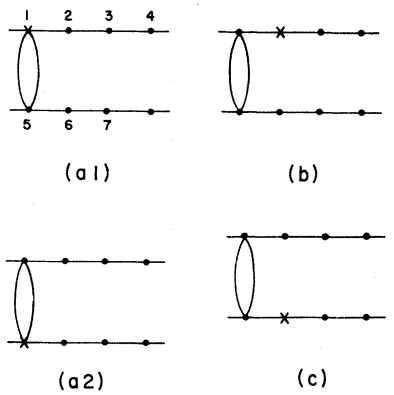

FIG. 2. Diagrammatical representation of interaction types $a1$, $a2$, b, and c.

(*i*) *Type* $a1$. In this type, the interaction (represented by a cross in Fig. 2) of the longitudinal photon is with a nucleon in cluster A (α cluster), which is involved in an intercluster nucleon-exchange process. Note that, for this type, there is no contribution from the no-exchange or direct term.

The kernel $I_x^{a1}(\vec{R}',\vec{R}'')$ has the form

$$I_x^{a1}(\vec{R}',\vec{R}'') = \binom{N_B}{x}^{-1}\mathfrak{N}_x(\vec{R}',\vec{R}'') \times\exp\{i\vec{q}\cdot[\omega'_{ax}\vec{R}' + \omega''_{ax}\vec{R}'' + \lambda_{ax}(\vec{R}'+\vec{R}'')] - \mu_{ax}q^2\}, \tag{47}$$

where

$$\mu_{ax} = \frac{1}{2(\alpha_A+\alpha_B)} - \frac{\nu_1^2}{4a_x} - \frac{\nu_2^2}{4c_x}, \tag{48}$$

$$\omega'_{ax} = -\frac{1}{2}\left(\frac{b_x}{a_x}\nu_1 - \frac{d_x}{c_x}\nu_2\right), \tag{49}$$

$$\omega''_{ax} = \frac{1}{2}\left(\frac{b_x}{a_x}\nu_1 + \frac{d_x}{c_x}\nu_2\right), \tag{50}$$

$$\lambda_{ax} = \frac{\mu_0(\alpha_A-\alpha_B)}{N(\alpha_A+\alpha_B)}, \tag{51}$$

with

$$b_x = \tfrac{1}{2}\mu_0, \tag{52}$$

$$d_x = -\frac{\mu_0(N_A\alpha_A + N_B\alpha_B)}{N^2\alpha_A\alpha_B(\alpha_A+\alpha_B)} \times[(N_B\alpha_A + N_A\alpha_B)(\alpha_A+\alpha_B) - x(\alpha_A-\alpha_B)^2], \tag{53}$$

$$\nu_1 = -1/[2(\alpha_A + \alpha_B)], \tag{54}$$

$$\nu_2 = \frac{N_A - N_B}{N(\alpha_A + \alpha_B)}. \tag{55}$$

(*ii*) *Type a*2. This type is similar to type *a*1, except that the virtual photon now interacts with a nucleon in cluster B (t cluster).

The kernel $I_x^{a2}(\vec{R}', \vec{R}'')$ is simply related to the kernel $I_x^{a1}(\vec{R}', \vec{R}'')$ by the equation

$$I_x^{a2}(\vec{R}', \vec{R}'') = I_x^{a1}(\vec{R}'', \vec{R}'). \tag{56}$$

(*iii*) *Type b*. Here the longitudinal photon interacts with a nucleon in cluster A, which is not involved in any intercluster nucleon-exchange process.

The kernels $I_0^b(\vec{R}', \vec{R}'')$ and $I_x^b(\vec{R}', \vec{R}'')$ are given by

$$I_0^b(\vec{R}', \vec{R}'') = \mathfrak{N}_0(\vec{R}', \vec{R}'')\exp[i\lambda_{b0}\vec{q}\cdot(\vec{R}' + \vec{R}'') - \mu_{b0}q^2] \tag{57}$$

with

$$\mu_{b0} = \frac{N_A{}^2\alpha_A + (N_A - 1)N_B\alpha_B}{4N_A\alpha_A(N_A\alpha_A + N_B\alpha_B)}, \tag{58}$$

$$\lambda_{b0} = \frac{N_B}{2N}, \tag{59}$$

and

$$I_x^b(\vec{R}', \vec{R}'') = \binom{N_B}{x}^{-1} \mathfrak{N}_x(\vec{R}', \vec{R}'') \times \exp[i\lambda_{bx}\vec{q}\cdot(\vec{R}' + \vec{R}'') - \mu_{bx}q^2] \tag{60}$$

with

$$\mu_{bx} = \frac{1}{4\alpha_A}\left(1 - \frac{N_B{}^2}{N^2\alpha_A c_x}\right), \tag{61}$$

$$\lambda_{bx} = \frac{N_B}{N\alpha_A}\left[\frac{N_A}{2N}(\alpha_A - \alpha_B) - \frac{d_x}{2c_x}\right]. \tag{62}$$

(*iv*) *Type c*. This type is similar to type *b*, except that the interacting nucleon is now in cluster B. Also, it should be noted that, for this type, there is no core-exchange (i.e., $x = N_B$) contribution.

The kernels $I_0^c(\vec{R}', \vec{R}'')$ and $I_x^c(\vec{R}', \vec{R}'')$ are given by

$$I_0^c(\vec{R}', \vec{R}'') = \mathfrak{N}_0(\vec{R}', \vec{R}'')\exp[i\lambda_{c0}\vec{q}\cdot(\vec{R}' + \vec{R}'') - \mu_{c0}q^2] \tag{63}$$

with

$$\mu_{c0} = \frac{N_B{}^2\alpha_B + N_A(N_B - 1)\alpha_A}{4N_B\alpha_B(N_A\alpha_A + N_B\alpha_B)}, \tag{64}$$

$$\lambda_{c0} = -\frac{N_A}{2N}, \tag{65}$$

and

$$I_x^c(\vec{R}', \vec{R}'') = \binom{N_B}{x}^{-1} \mathfrak{N}_x(\vec{R}', \vec{R}'') \times \exp[i\lambda_{cx}\vec{q}\cdot(\vec{R}' + \vec{R}'') - \mu_{cx}q^2] \tag{66}$$

with

$$\mu_{cx} = \frac{1}{4\alpha_B}\left(1 - \frac{N_A{}^2}{N^2\alpha_B c_x}\right), \tag{67}$$

$$\lambda_{cx} = \frac{N_A}{N\alpha_B}\left[\frac{N_B}{2N}(\alpha_A - \alpha_B) + \frac{d_x}{2c_x}\right]. \tag{68}$$

It should be pointed out that, as mentioned in Ref. 29, the diagrams shown in Fig. 2 are considered to include implicitly all other diagrams which contain additional exchange loops not involving the interacting nucleon. Thus, diagrams drawn in Fig. 3 belong also to type *a*1 and type *b*, and do not need to be explicitly shown.

All the integrals appearing in Eqs. (30), (43), and (44) can be evaluated by using the following general formulas:

$$\int G_\mu^*(\vec{R}')\exp(i\gamma\vec{q}\cdot\vec{R}')G_\mu(\vec{R}')d\vec{R}' = C(011; 0\mu\mu)C(011; 000)\int [f_G(R')]^2 j_0(\gamma qR')dR' - 5C(211; 0\mu\mu)C(211; 000)\int [f_G(R')]^2 j_2(\gamma qR')dR' \tag{69}$$

with j_λ being a spherical Bessel function, and

$$\int G_\mu^*(\vec{R}')K(\vec{R}', \vec{R}'')\exp[i\vec{q}\cdot(\alpha\vec{R}' + \beta\vec{R}'')]G_\mu(\vec{R}'')d\vec{R}'d\vec{R}'' = \sum_L \sum_{l_\alpha} \sum_{l_\beta} (2l_\alpha + 1)(2l_\beta + 1)i^{l_\alpha + l_\beta}C(Ll_\alpha 1; \mu 0\mu)C(Ll_\alpha 1; 000) \times C(l_\beta 1L; 0\mu\mu)C(l_\beta 1L; 000)\int f_G(R')k_L(R', R'')j_{l_\alpha}(\alpha qR')j_{l_\beta}(\beta qR'')f_G(R'')dR'dR''. \tag{70}$$

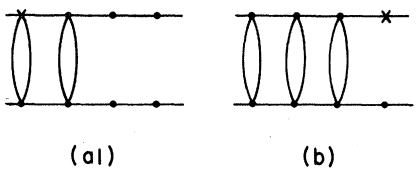

FIG. 3. Other type-$a1$ and type-b diagrams.

In deriving the above equation, we have used the expansion

$$K(\vec{R}',\vec{R}'')=\frac{1}{R'R''}\sum_{L}\sum_{M}k_L(R',R'')Y_L^M(\hat{R}')Y_L^{M*}(\hat{R}''). \tag{71}$$

Also, the triple summation in Eq. (70) is rather simple to carry out. For a fixed value of L, one obtains nonzero contributions only when l_α and l_β take on values equal to $(L\pm1)$. In the actual calculation, we have used L values from 0 up to a maximum L_M, which is around 10 for the largest q^2 value considered in our present study.

III. RESULTS

In the $t+\alpha$ system where the nucleon-number difference of the interacting nuclei is small, it was shown that core-exchange effects have major significance and can be approximately represented by a rather strong effective internuclear interaction which is not only parity-dependent but also long-ranged.[29] As a consequence, it is found here that, because of the appearance of the core-exchange ($x=3$) type-b term in I_p of Eq. (45), the value of L_M must be chosen to be quite large at high momentum transfer. This is demonstrated in Fig. 4, where we show the convergence behavior of F_{ch}^2 as L_M increases. As is seen, the value of L_M necessary for an accurate determination of F_{ch}^2 should be at least 6 for $q^2=3$ fm^{-2} and 8 for $q^2=6$ fm^{-2}.

In Fig. 5, we show by the solid curve the calculated F_{ch}^2 values for q^2 up to 7 fm^{-2}. The empirical data shown are those of Suelzle *et al.*[15] From this figure, one sees that there is a rather satisfactory agreement over the whole range of q^2 studied. Considering the fact that in our present investigation the charge form factor is calculated straightforwardly from a resonating-group wave function obtained in a nuclear-structure study and no adjustments are made, we must view this as an important development in establishing the soundness of the resonating-group approach to solve problems at least in light nuclear systems.

Contributions from C0 and C2 interactions are also depicted separately in Fig. 5. Here one finds that the C0 contribution is dominant for low-q^2

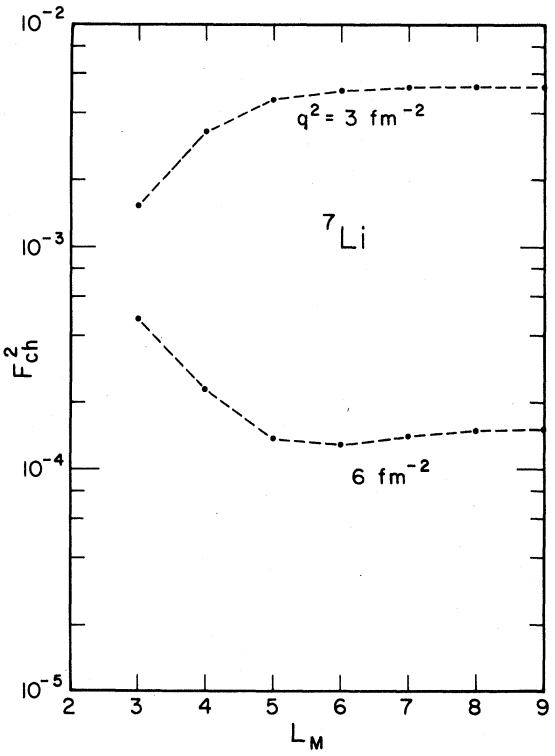

FIG. 4. Convergence behavior of F_{ch}^2 as a function of L_M for $q^2=3$ and 6 fm^{-2}.

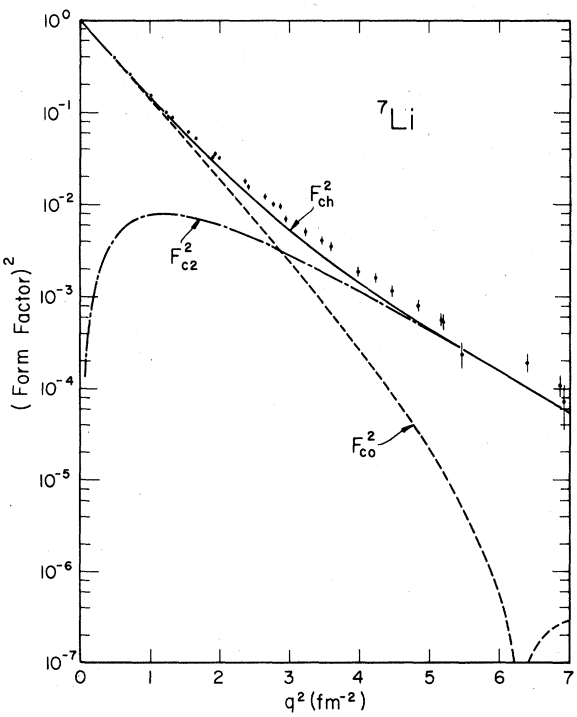

FIG. 5. Comparison of calculated and empirical results for F_{ch}^2. Contributions from C0 and C2 interactions are also shown.

values smaller than about 2 fm^{-2}. At high momentum transfers, the contribution comes instead mainly from the $C2$ term, which indicates that the ^{7}Li nucleus has a large intrinsic quadrupole deformation in its ground state. This latter feature is correctly contained in the wave function used in our calculation, because it is one of the main advantages of a resonating-group or cluster-model calculation that collective behavior in the form of nucleon clustering is generally taken into account in an adequate manner.

Using Eqs. (24) and (25) and the low-q^2 behavior of the form factors, we determine the rms charge radius R_{ch} and the spectroscopic quadrupole moment Q. The results are

$$R_{ch} = 2.44 \text{ fm} \tag{72}$$

and

$$Q = -3.70 \text{ fm}^2 . \tag{73}$$

Comparing with the empirical values for R_{ch} of 2.35 ± 0.10 fm obtained by a model-independent analysis[30] of experimental data at low momentum transfers less than about 1 fm^{-1} and 2.39 ± 0.03 fm obtained by an oscillator shell-model analysis[15] of higher-q^2 data, we conclude that our result obtained here is quite good. As for the spectroscopic quadrupole moment, the experimentally determined value[19] is -3.66 ± 0.03 fm^2, which agrees well with our result given by Eq. (73).

From Fig. 5, one also notes that the calculated curve for F_{ch}^2 lies slightly below the data points. The reasons for this discrepancy are likely as follows.

(i) The wave function used was the result of a single-channel resonating-group calculation with only the $t+\alpha$ cluster configuration taken into account. Because of the rather low compressibilities of the clusters involved, the specific distortion effect[1] was anticipated to be relatively unimportant[31,32] and, hence, has not been explicitly considered. However, it is certainly evident that this effect will influence, although not to a large extent, the behavior of the wave function in the strong-interaction region and, thereby, affect somewhat the result of the form-factor calculation. Therefore, it will be worthwhile to carry out a further resonating-group calculation which includes both $t+\alpha$ and $n+{}^6$Li cluster configurations in the formulation. Since in ^{7}Li the $n+{}^6$Li threshold occurs at a higher energy than the $t+\alpha$ threshold, the relative-motion part of the $n+{}^6$Li component will drop more sharply in the surface region of the compound system than that of the $t+\alpha$ component. Consequently, it would be reasonable to expect that, with such a more refined wave function, the calculated magnitudes of R_{ch} and Q will turn out to be slightly smaller than those given by Eqs. (72) and (73) and thus agree even better with empirically determined results.

(ii) In the q^2 region up to about 6 fm^{-2}, the values of the body form factor for the α particle, calculated with the wave function of Eq. (4), agree quite well with those empirically determined.[33] On the other hand, the body form factor for the triton, calculated with the wave function of Eq. (5), is smaller than the empirical result by about 10% at $q^2 = 3$ fm^{-2} and about 40% at $q^2 = 6$ fm^{-2}.[33] This indicates, therefore, that to obtain a better agreement with ^{7}Li empirical charge form-factor values, one may need to further perform a resonating-group calculation which employs a more flexible triton wave function (e.g., a two-Gaussian function) than the one we adopt here.

Improved calculations[34] incorporating these particular features can be readily carried out within the resonating-group framework by using the CGCT mentioned above. The results obtained should provide us with additional information concerning the complicated structure of the nucleus ^{7}Li in its ground state.

The behavior of the quantities F^p_{C0} and F^p_{C2} for the proton distribution and the quantities F^n_{C0} and F^n_{C2} for the neutron distribution, defined as

$$F^i_{C0} = \tfrac{1}{2}(F^i_{3/2} + F^i_{1/2}) \quad (i = p \text{ or } n) \tag{74}$$

and

$$F^i_{C2} = \tfrac{1}{2}(F^i_{3/2} - F^i_{1/2}) \quad (i = p \text{ or } n), \tag{75}$$

is shown in Fig. 6. From this figure, one may easily infer that the proton and neutron distributions possess rather different characteristics. Compared to the proton distribution, the neutron distribution has a larger rms radius and is more

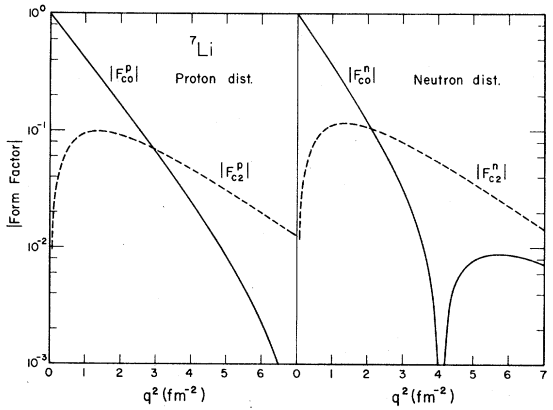

FIG. 6. Magnitudes of form factors F^p_{C0}, F^p_{C2}, F^n_{C0}, and F^n_{C2} for proton and neutron distributions in ^{7}Li.

intrinsically deformed. Based on the viewpoint of the cluster model,[1] this type of difference may be explained as arising from the fact that the ratio of neutron-to-proton number in the lighter cluster (i.e., t cluster) is larger than that in the heavier cluster (i.e., α cluster).

Together with the observation that the ^{3}He separation energy in the ground state of ^{7}Be is appreciably smaller than the triton separation energy in the ground state of ^{7}Li, the above discussion indicates that the charge form factors of ^{7}Be and ^{7}Li are likely to be substantially different. To verify this, one needs, of course, to perform an elastic electron-scattering experiment on the nucleus ^{7}Be. Quite clearly, this will be an interesting experiment, the result of which will yield considerable information concerning the electromagnetic structure of the seven-nucleon system. However, because of the unstable nature of ^{7}Be, with a half-life of about 53 days, we fully expect that to successfully carry out such an experiment will not be a simple task.

IV. CONCLUSION

In this investigation, we calculate the charge form factor of ^{7}Li by using a wave function which is obtained from a single-channel $t+\alpha$ resonating-group study. The main characteristics are the following: (i) a totally antisymmetric wave function is used, (ii) the c.m. motion is correctly considered, and (iii) no adjustable parameters are involved. Both $C0$ and $C2$ contributions are included in the calculation, and proton and neutron distributions are separately taken into account. The result shows that a good agreement between theory and experiment can be obtained. The calculated values for the rms charge radius and spectroscopic quadrupole moment are equal to 2.44 fm and -3.70 fm^2, respectively, which agree very well with empirically determined values.

At present, there exist also $C0$ form-factor calculations with resonating-group wave functions for the nuclei ^{6}Li,[35] ^{12}C,[36] and ^{20}Ne.[37] In all these cases, satisfactory agreement with experiment has been obtained. Together with the interesting results obtained here, our conviction is reinforced that the resonating-group method is a sound microscopic approach to solving nuclear problems and should be extensively used, especially in light- and medium-weight nuclear systems.

The successful conclusion of this investigation indicates to us that we should proceed to examine other electromagnetic and also weak-interaction problems in the seven-nucleon system. These problems include the radiative-capture reaction of ^{3}He by ^{4}He, the $M1$ and $M3$ form-factor study in ^{7}Li,[38] the electron capture of ^{7}Be, and so on. Among these, especially the radiative-capture calculation[39] should be carried out soon, because it is crucial to the solution of the solar-neutrino problem, which is an outstanding puzzle at the present moment.

ACKNOWLEDGMENTS

Two of us (H. K. and Q.K.K.L.) wish to thank Professor B. F. Bayman and Professor P. J. Ellis for the kind hospitality extended to them at the School of Physics, University of Minnesota. This research was supported in part by the U. S. Department of Energy under Contract No. DOE/DE-AC02-79 ER 10364.

---

*Present address.
†Permanent address.

[1] K. Wildermuth and Y. C. Tang, A. *Unified Theory of the Nucleus* (Vieweg, Braunschweig, 1977).
[2] Y. C. Tang, M. LeMere, and D. R. Thompson, Phys. Rep. 47, 167 (1978).
[3] K. Wildermuth and E. J. Kanellopoulos, Rep. Prog. Phys. 42, 1719 (1979).
[4] K. Ikeda, R. Tamagaki, S. Saito, H. Horiuchi, A. Tohsaki-Suzuki, and M. Kamimura, Prog. Theor. Phys. (Suppl) 62, 1 (1977).
[5] T. Kaneko and H. Kanada, Prog. Theor. Phys. 57, 1277 (1977).
[6] D. Baye, P. H. Heenan, and M. Libert-Heinemann, Nucl. Phys. A308, 229 (1978).
[7] H. Friedrich, K. Langanke, and A. Weiguny, Phys. Lett. 63B, 125 (1976).
[8] H. H. Hackenbroich, T. H. Seligman, and W. Zahn, Nucl. Phys. A259, 445 (1976).
[9] W. Sünkel and K. Wildermuth, Phys. Lett. 41B, 439 (1972).
[10] T. Matsuse, M. Kamimura, and Y. Fukushima, Prog. Theor. Phys. 53, 706 (1975).
[11] M. LeMere, Y. C. Tang, and D. R. Thompson, Phys. Rev. C 14, 23 (1976).
[12] T. Tomoda and A. Arima, in *Proceedings of the* INS-IPCR *Symposium on Cluster Structure of Nuclei and Transfer Reactions Induced by Heavy Ions, Tokyo, 1975,* edited by H. Kamitsubo, I. Kohno, and T. Marumori (The Institute of Physical and Chemical Research, Wako-shi, Saitma, Japan, 1975), p. 90.
[13] R. D. Furber, Ph.D. thesis, University of Minnesota, 1976.
[14] In fact, with the introduction of a phenomenological imaginary potential [see Ref. 13 and R. E. Brown, *Proceedings of the Third International Conference on*

Clustering Aspects of Nuclear Structure and Nuclear Reactions (AIP, New York, 1978)], it is even possible to fit quite well all the available higher-energy differential cross-section and polarization data.

[15]L. R. Suelzle, M. R. Yearian, and H. Crannell, Phys. Rev. 162, 992 (1967).

[16]M. E. Rose, *Elementary Theory of Angular Momentum* (Wiley, New York, 1957).

[17]J. A. Koepke, R. E. Brown, Y. C. Tang, and D. R. Thompson, Phys. Rev. C 9, 823 (1974).

[18]D. R. Thompson and Y. C. Tang, Phys. Rev. C 12, 1432 (1975); 13, 2597 (1976).

[19]F. Ajzenberg-Selove, Nucl. Phys. A320, 1 (1979).

[20]B. Buck, H. Friedrich, and C. Wheatley, Nucl. Phys. A275, 246 (1976).

[21]S. Saito, S. Okai, R. Tamagaki, and M. Yasuno, Prog. Theor. Phys. 50, 1561 (1973).

[22]T. Matsuse and M. Kamimura, Prog. Theor. Phys. 49, 1765 (1973).

[23]T. Fliessbach, Z. Phys. A 272, 39 (1975).

[24]L. I. Schiff, Phys. Rev. 96, 765 (1954).

[25]L. I. Schiff, Phys. Rev. 133, B802 (1964).

[26]T. Janssens, R. Hofstadter, E. B. Hughes, and M. R. Yearian, Phys. Rev. 142, 922 (1966).

[27]M. LeMere, Ph.D. thesis, University of Minnesota, 1977.

[28]D. R. Thompson, M. LeMere, and Y. C. Tang, Phys. Lett. 69B, 1 (1977).

[29]M. LeMere, D. J. Stubeda, H. Horiuchi, and Y. C. Tang, Nucl. Phys. A320, 449 (1979).

[30]F. A. Bumiller, F. R. Buskirk, J. N. Dyer, and W. A. Monson, Phys. Rev. C 5, 391 (1972).

[31]M. LeMere, R. E. Brown, Y. C. Tang, and D. R. Thompson, Phys. Rev. C 12, 1140 (1975).

[32]The calculation of Mihailović and Poljsak [M. V. Mihailović and M. Poljsak, Nucl. Phys. A311, 377 (1978)] indicates that this is indeed the case. There it was found that the addition of the $n+{}^6$Li cluster configuration into a single-channel $t+\alpha$ resonating-group calculation decreases the ground-state energy by only 0.32 MeV, which is not a large amount.

[33]Y. C. Tang and R. C. Herndon, Phys. Lett. 18, 42 (1965).

[34]Unfortunately, the wave function obtained by Mihailović and Poljsak [see Ref. 32] is not appropriate for use in a detailed form-factor study, because an unrealistic assumption of equal oscillator width parameters for all the clusters involved has been adopted in their calculation. With the computational technique used by these authors, such an assumption is necessary in order to avoid the occurrence of spurious c.m. motion in the formulation.

[35]H. Stöwe, H. H. Hackenbroich, and H. Hutzelmeyer, Z. Phys. 247, 95 (1971).

[36]M. Kamimura, Fizika (Zagreb), 9 (Suppl. 3), 159 (1977).

[37]Y. Fukushima, M. Kamimura, and T. Matsuse, Prog. Theor. Phys. 55, 1310 (1976).

[38]R. E. Rand, R. Frosch, and M. R. Yearian, Phys. Rev. 144, 859 (1966).

[39]The calculation by Tombrello and Parker [T. A. Tombrello and P. D. Parker, Phys. Rev. 131, 2582 (1963)] is a macroscopic type containing adjustable parameters.